The bolometer diagnostic at the stellarator Wendelstein 7-X

P. Hacker[1,2], D. Zhang[1], R. Burhenn[1]

[1]Max Planck Institute for Plasma Physics, Wendelsteinstr. 1, D-17491 Greifswald, Germany

[2]Ernst-Moritz-Arndt University Greifswald, Domstr. 11, D-17489 Greifswald, Germany

May 14th, 2018

This work has been carried out within the framework of the EUROfusion Consortium and has received funding from the Euratom research and training programme 2014-2018 under grant agreement No. 633053. The views and opinions expressed herein do not necessarily reflect those of the European Commission.

Contents

Goals

What is the bolometer at W7-X?

– a two camera system using metal film resistive detector arrays to measure plasma radiation based on thermal effects

Goals:

1. - globale power balance: investigation of total radiation power loss, mainly from impurities, and its distribution
2. - local power balance: radiation profiles for transport studies (using tomographic inversion)

Construction

- multi-camera system with 113 channels combined: 32@HBCm and 2 x 24@VBC subdetectors (+ differently coated/filtered channels)

HBCm

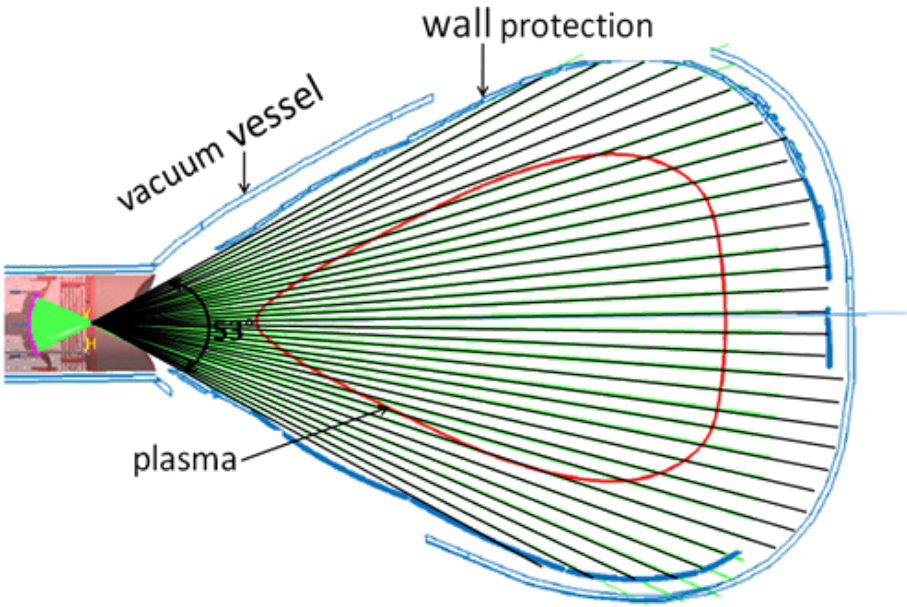

VBCr/VBCl

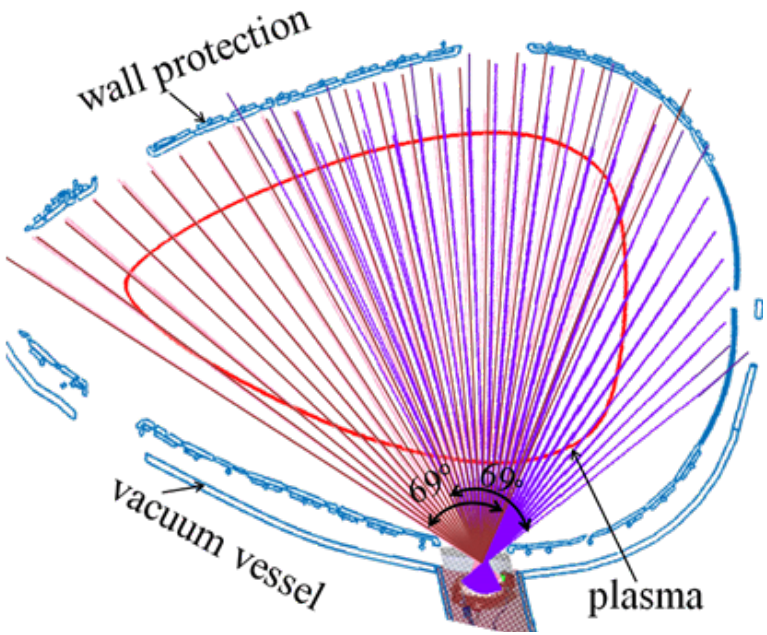

(Lines of sight with individual apertures, retracted into the vacuum vessel)

Construction

- multi-camera system with 113 channels combined: 32@HBCm and 2 x 24@VBC subdetectors (+ differently coated/filtered channels)

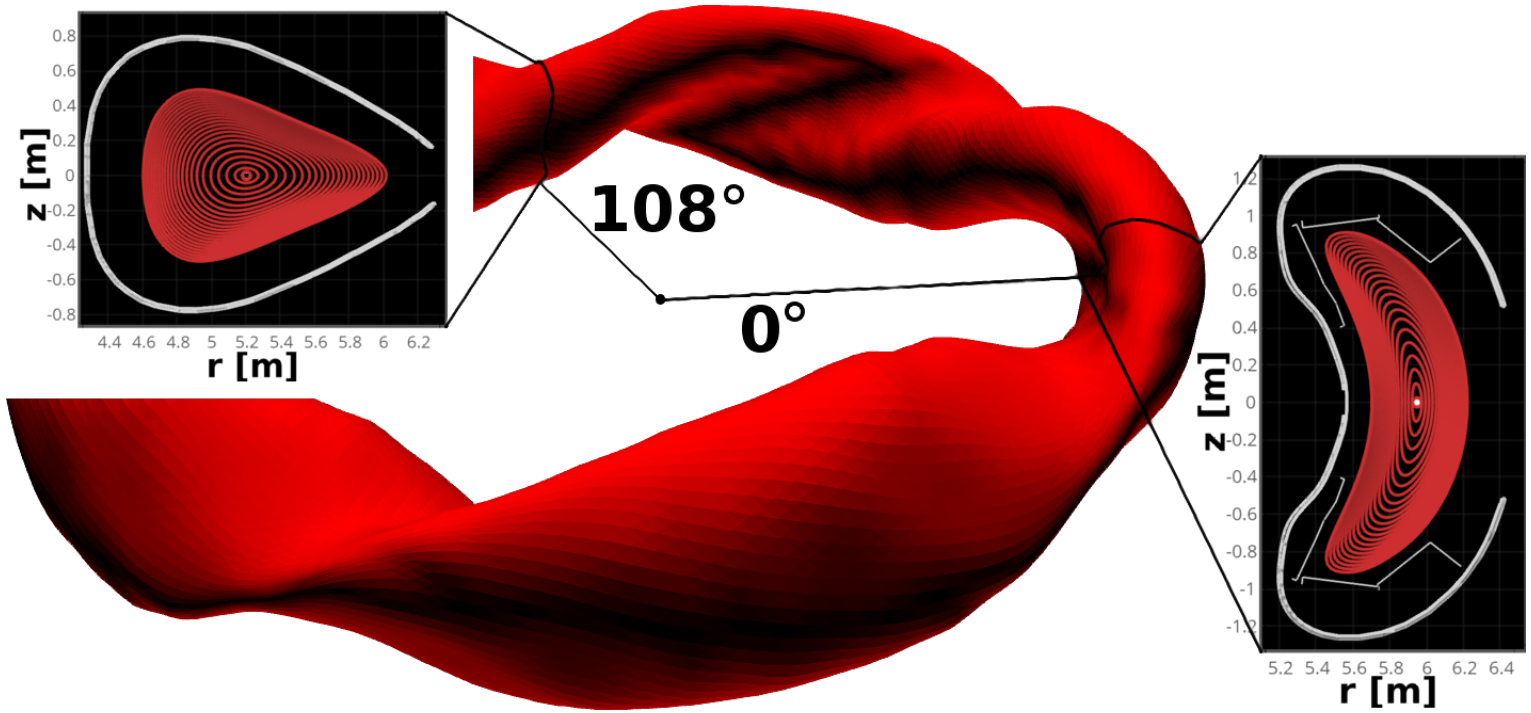

(W7-X equilibrium fluxsurfaces from VMEC)

Construction

- multi-camera system with 113 channels combined: 32@HBCm and 2 x 24@VBC subdetectors (+ differently coated/filtered channels)

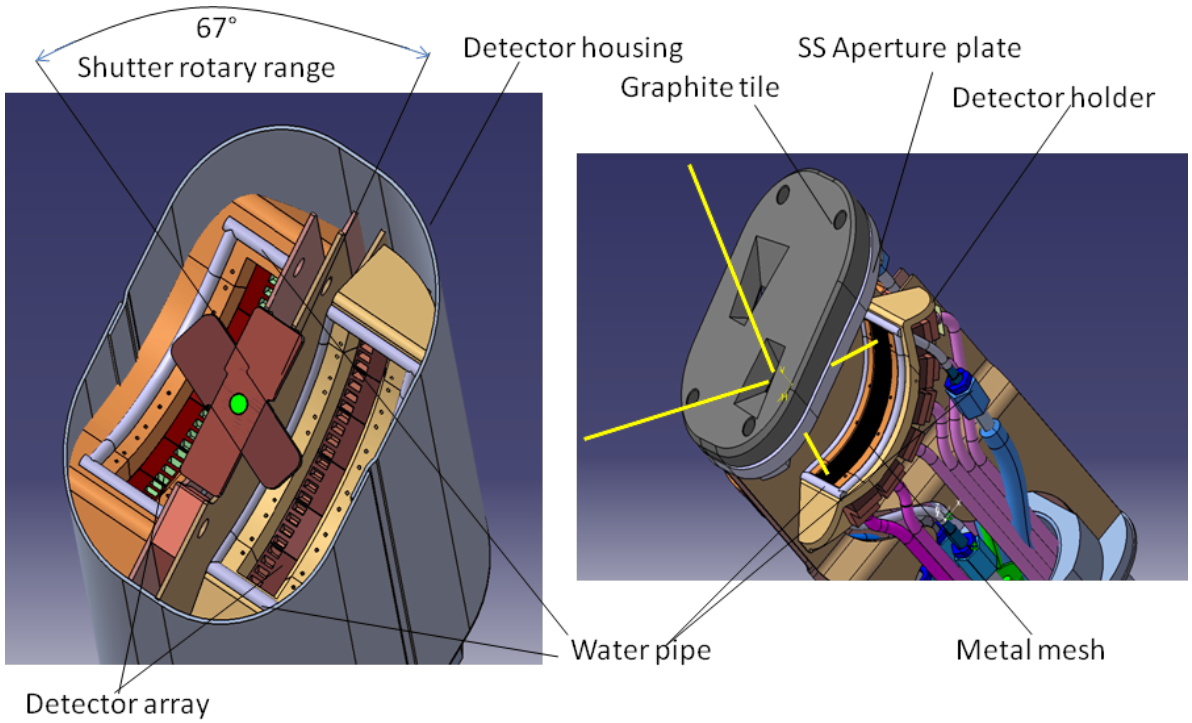

(Camera head (VBCl/r) construction)

Performance

- spatial resolution of 5 cm & temporal resolution of 0.8 ms to 1.6 ms
- detectors of 5 µm thick gold-foil absorbers with carbon coating on 1.5 µm Si_3N_4 substrate and gold meander for 200 nW resolution between 600 nm to 0.2 nm

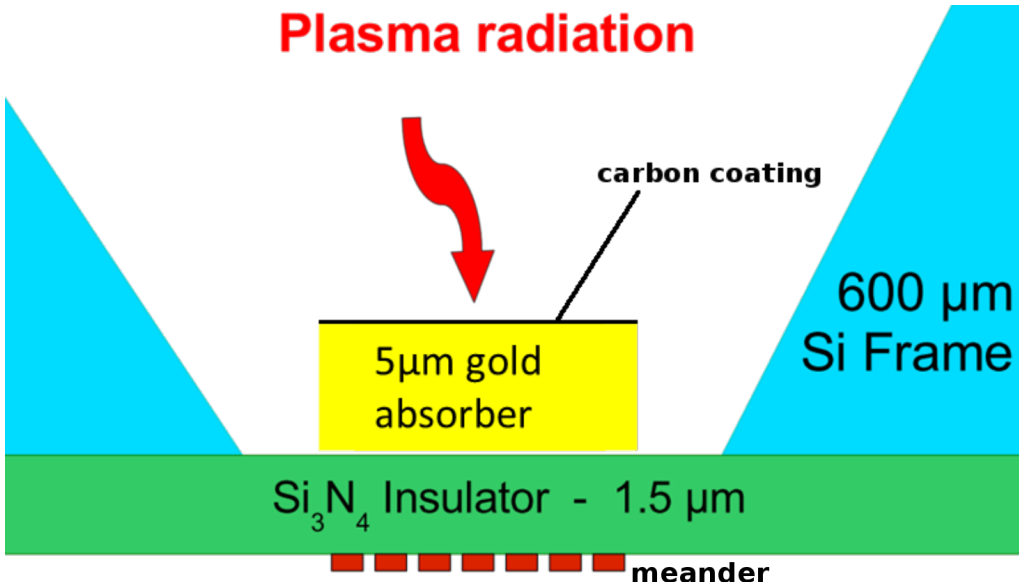

(Single detector channel scheme with holder)

Performance

- spatial resolution of 5 cm & temporal resolution of 0.8 ms to 1.6 ms
- detectors of 5 µm thick gold-foil absorbers with carbon coating on 1.5 µm Si_3N_4 substrate and gold meander for 200 nW resolution between 600 nm to 0.2 nm

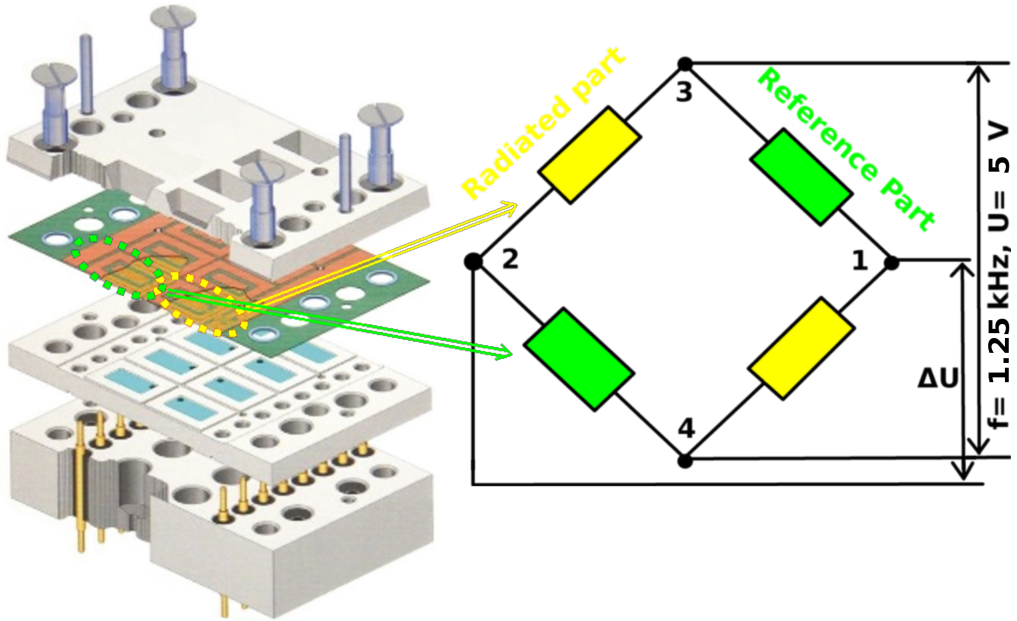

([Left] Detector array of one head with reference [Right] Wheatstone bridge, radiated (green) and un-exposed (yellow) parts)

Calibration & Calculation

Design criteria

- water cooled elements (front plates) for 30 min steady state operation
- ECRH stray radiation ($\sim 10\,\mathrm{kW\,m^{-2}}$) screening by wire-mesh and absorption by ceramic coating inside the camera enclosure

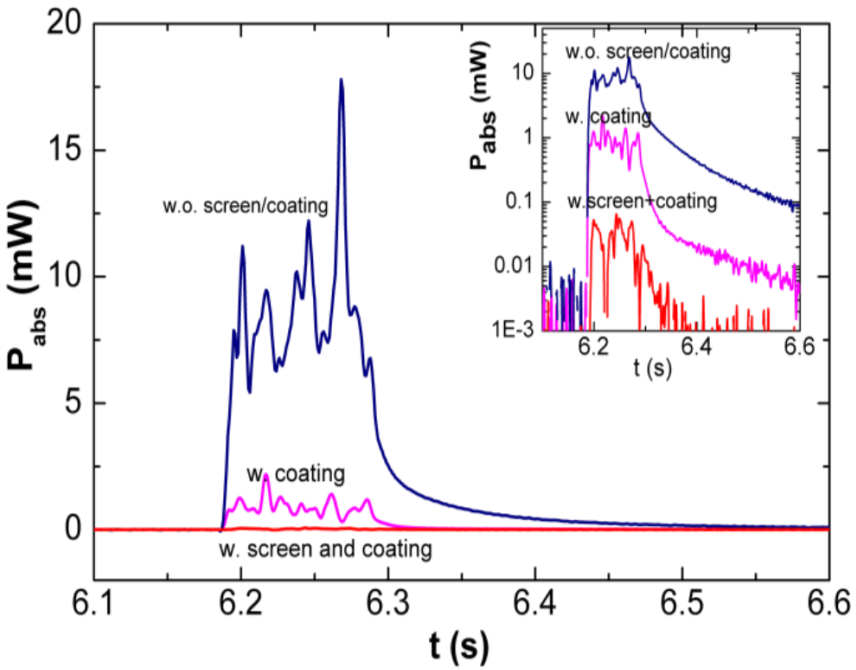

(Bolometer prototype in strong microwave background of MISTRAL)

$\ll$ 1% microwave power flux
&
53% optical transmissivity

Equations

Plasma radiation

$$P_{rad,bolo} \propto \sum_Z n_e \cdot n_Z \cdot L_Z$$

- L_Z: line radiation function of impurity Z
  $\ldots = f\,(T_e,\ T_i,\ T_Z,\ wall\ material/conditions,\ \ldots)$

Equations

Plasma radiation

$$P_{rad,bolo} \propto \sum_Z n_e \cdot n_Z \cdot L_Z$$

$$\ldots = \frac{V_{P,tor}}{V_{cam}} \cdot \sum_{ch} \frac{V_{ch}}{K_{ch}} \cdot \frac{P_{ch}}{f_{OT}}$$

- V_{ch}: polygon volume of detector ch
- $V_{P,tor}$: estimated plasma volume (EMC3 simulation)
- K_{ch}: geometrical factor for channel ch

Plasma radiation

$$P_{rad,bolo} \propto \sum_Z n_e \cdot n_Z \cdot L_Z$$

$$\ldots = \frac{V_{P,tor}}{V_{cam}} \cdot \sum_{ch} \frac{V_{ch}}{K_{ch}} \cdot \frac{P_{ch}}{f_{OT}}$$

Bolometer equation:

$$P_{ch} = \frac{2}{U_{eff}} \cdot (R_{ch} + 2R_C) \cdot \kappa_{ch} \sqrt{g_C} \cdot \left(\tau_{ch} \frac{\mathrm{d}(\Delta U)}{\mathrm{d}t} + f_\tau \cdot (\Delta U) \right)$$

- $\Delta U \propto \Delta T$ the change in absorber temperature
- U_{eff}: voltage divider between foil and reference

Equations

Plasma radiation

$$P_{rad,bolo} \propto \sum_Z n_e \cdot n_Z \cdot L_Z$$

$$\ldots = \frac{V_{P,tor}}{V_{cam}} \cdot \sum_{ch} \frac{V_{ch}}{K_{ch}} \cdot \frac{P_{ch}}{f_{OT}}$$

Bolometer equation:

$$P_{ch} = \frac{2}{U_{eff}} \cdot (R_{ch} + 2R_C) \cdot \kappa_{ch} \sqrt{g_C} \cdot \left(\tau_{ch} \frac{\mathrm{d}(\Delta U)}{\mathrm{d}t} + f_\tau \cdot (\Delta U) \right)$$

- $\tau,\ \kappa,\ R$: cooling time, heat capacity and resistance of foil
- $R_C,\ C_{cab}$: electrical connector properties
- f_{bridge}: Wheatstone bridge scaling factor

Preliminary results (OP1.2a)

steady state vs. collapse

Channel signals (steady state)

voltage

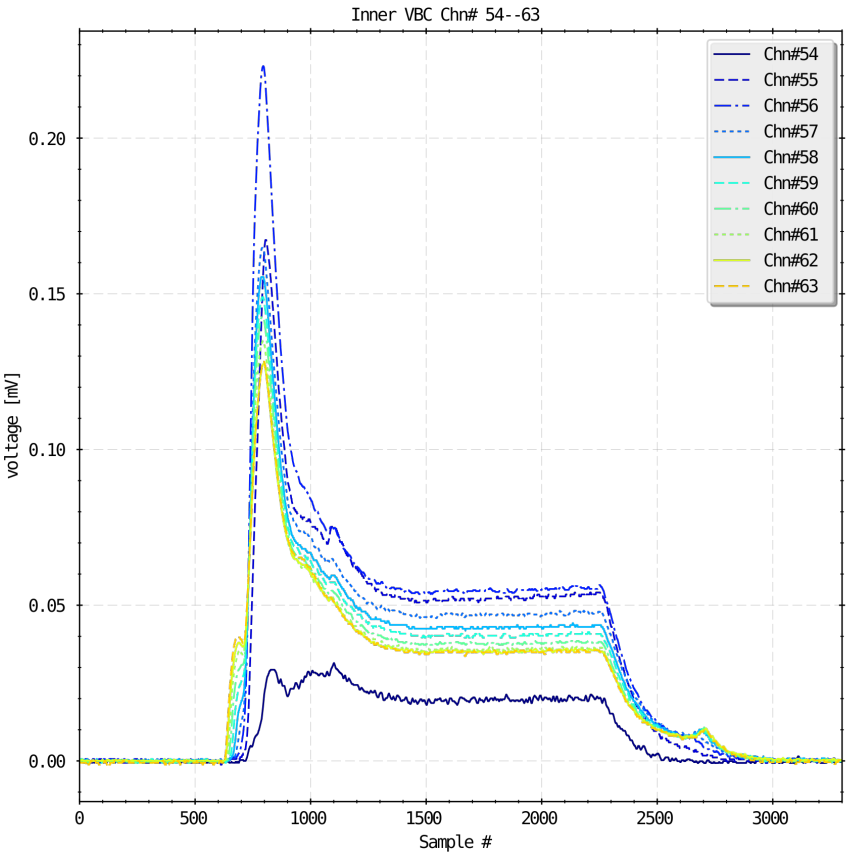

power

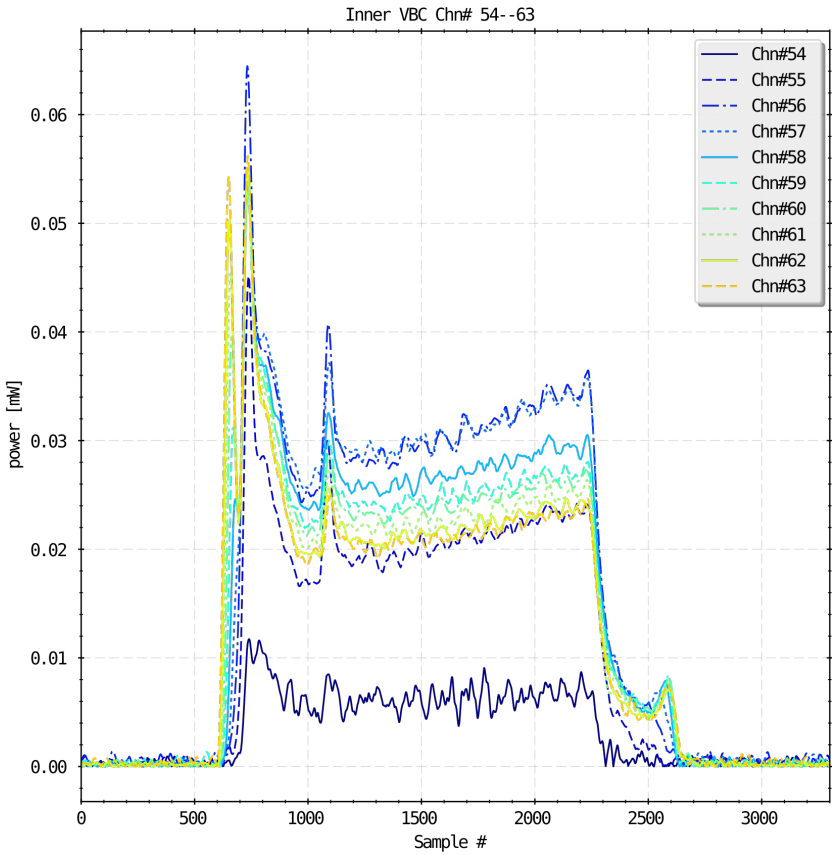

Discharge XP.20171114.52: Selection of channels from the VBCI (innermost part), both raw voltage and calculated power P_{ch}

steady state vs. collapse

Total radiated power (steady state)

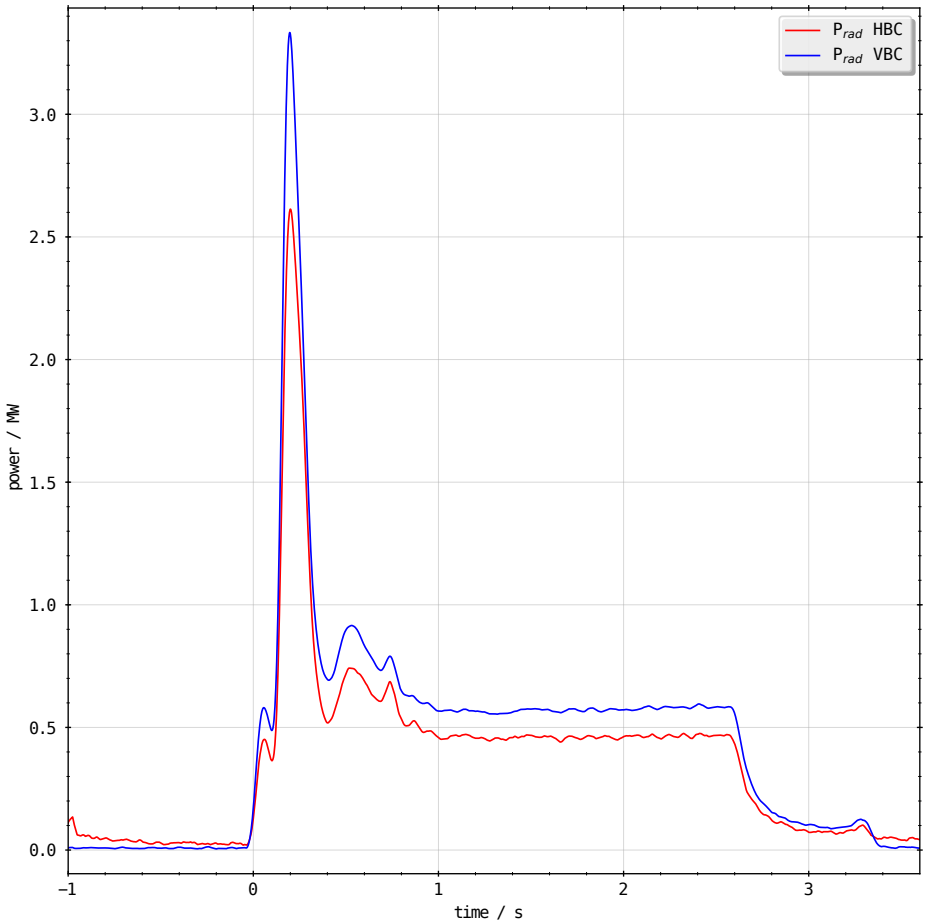

Discharge XP.20171114.52: Full radiated power of both cameras/camera arrays according to previous equations.

steady state vs. collapse

Discharge overview (steady state)

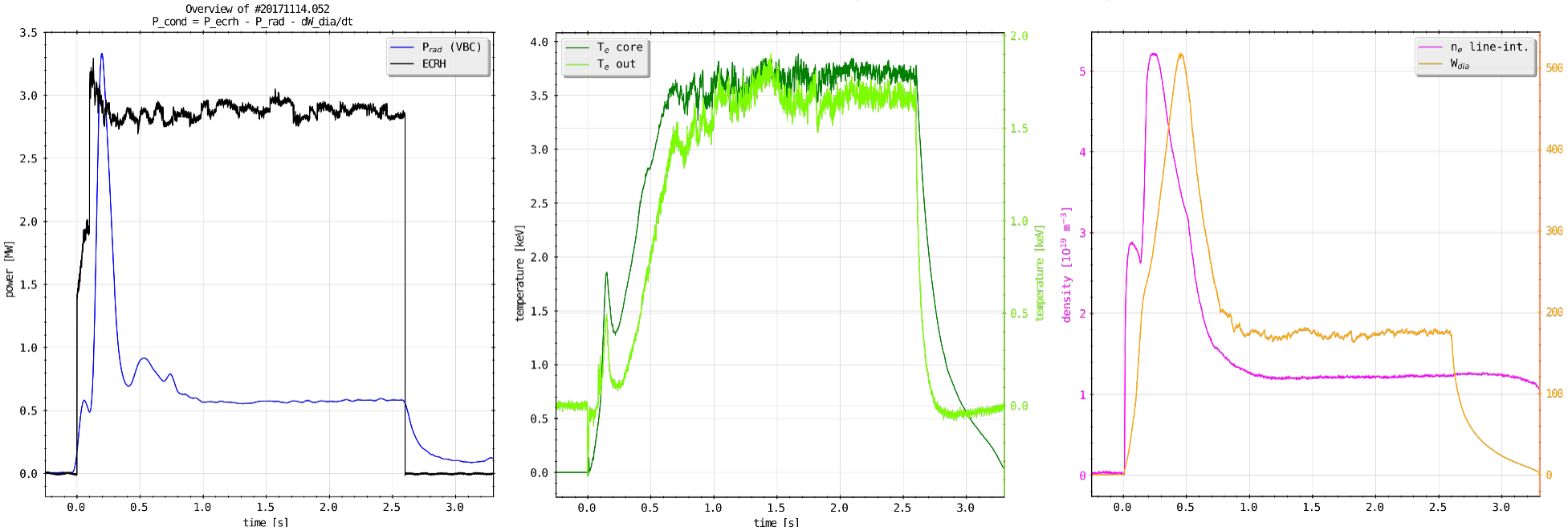

Discharge XP.20171114.52: Experiment parameters for the same discharge (2.7s, terminated).

steady state vs. collapse

Discharge overview (radiative collapse)

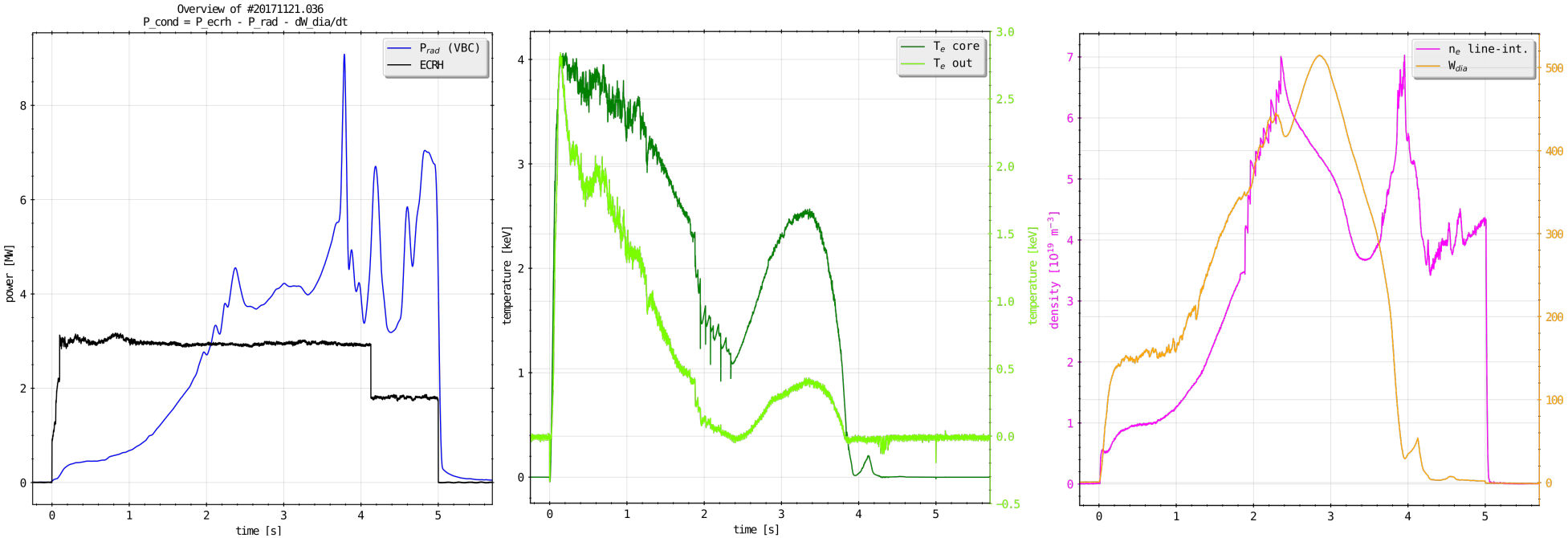

Discharge XP.20171121.36: Discharge properties. Similar setup as for previous discharge, but with frozen H_2 pellet injection. Collapse around 2.9s.

steady state vs. collapse

Radiation profile over effective radius (steady state)

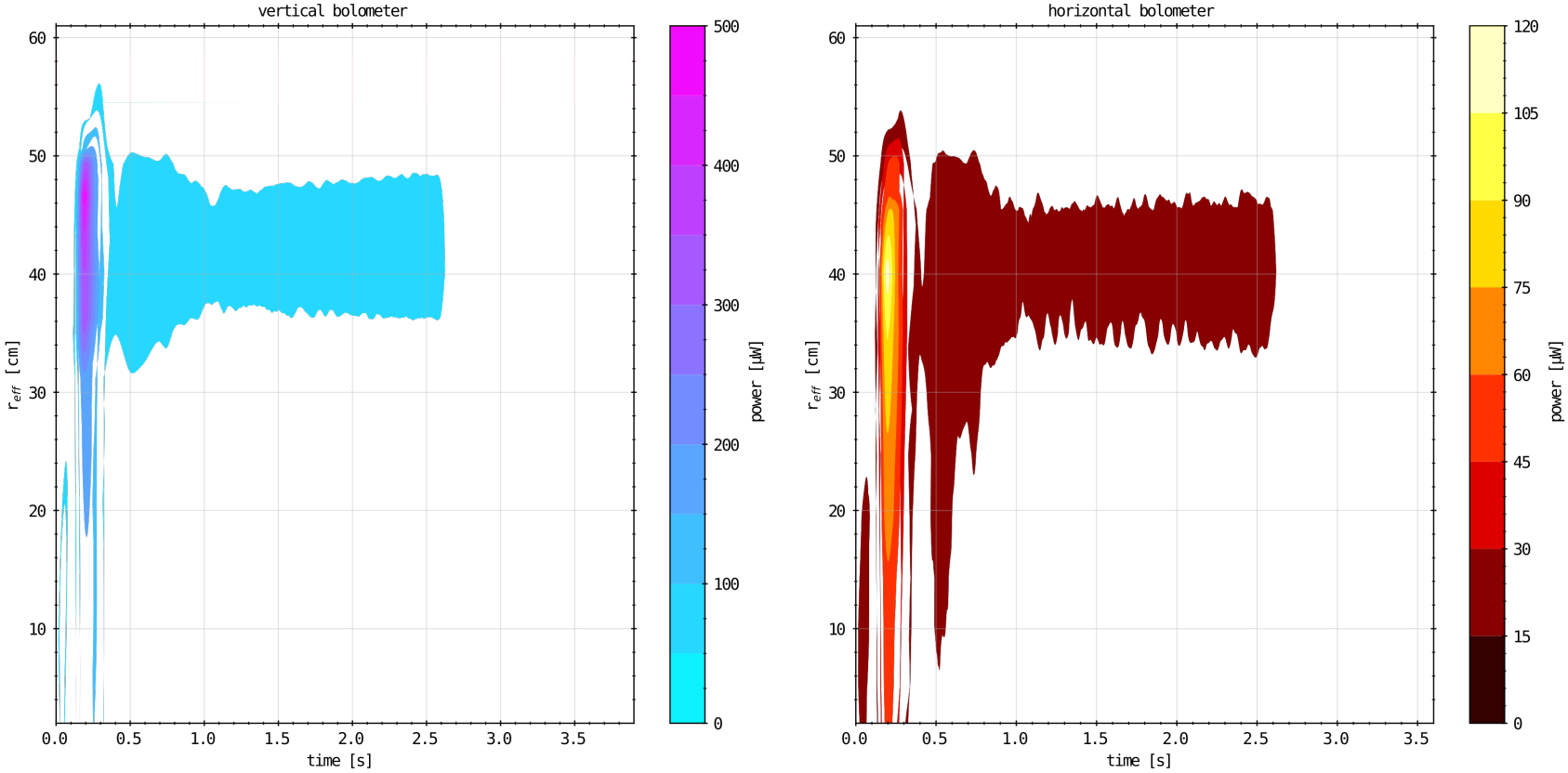

Discharge XP.20171114.52: Channel power vs. effetive plasma radius, e.g. $\rho eff = \sqrt{\Psi}$ the distance from the magnetic field center, both cameras.

steady state vs. collapse

Radiation profile over effective radius (collapse)

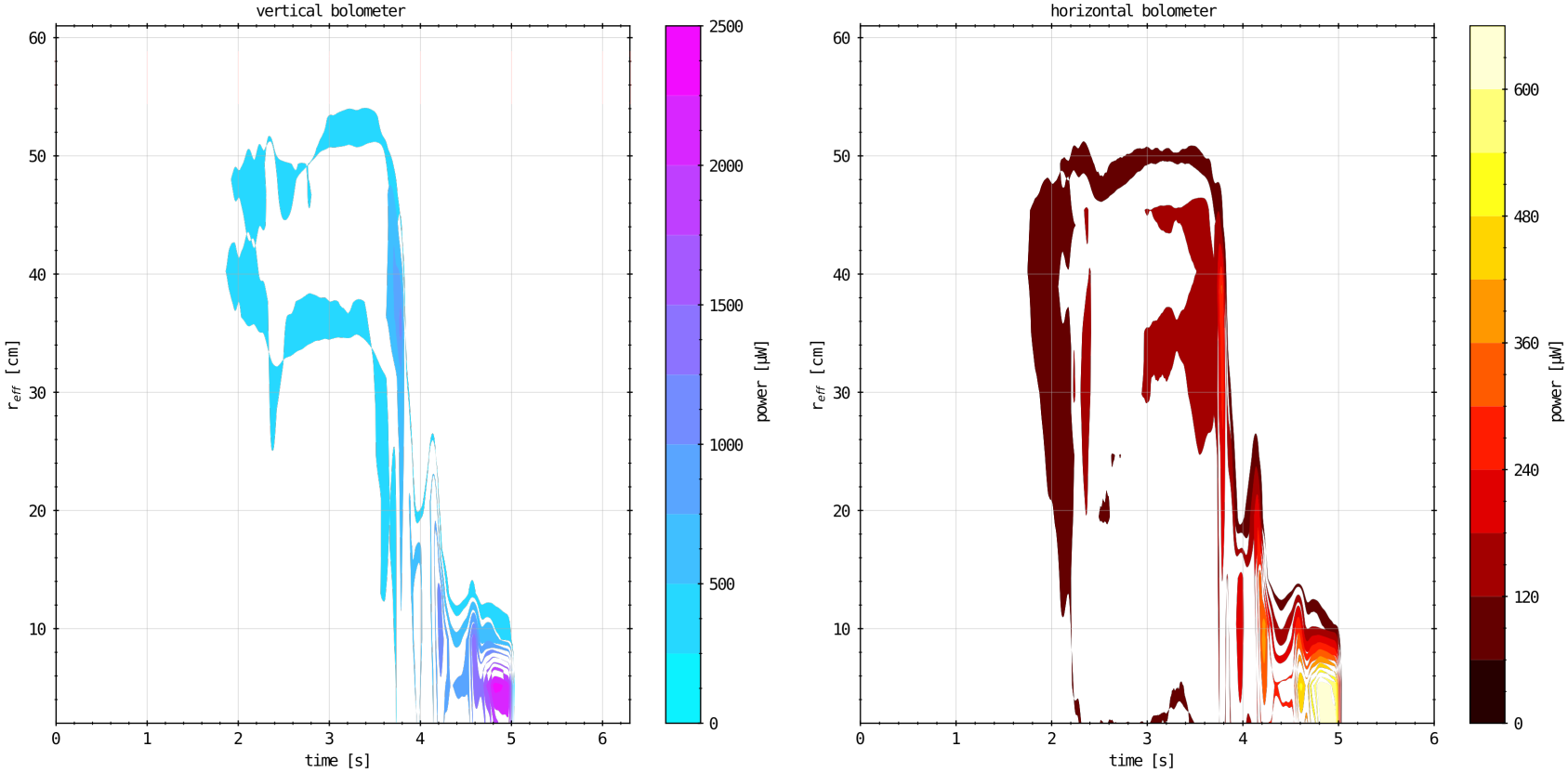

Discharge XP.20171121.26: Channel power vs. effetive plasma radius with radiative collapse.

Outlook

Goals

1.- Verifying and improve the evaluation of measurement data

2.- instantaneous/direct tomographic inversion after discharge
$\Rightarrow$ investigation of impurity transport processes and discharge feedback

3.- providing feedback signal for other diagnostics/CoDaC through fast (5 ms) calculation of P_{rad} estimate

End

Thank you for your attention!
Now: questions.

Bibliography

- "Design Criteria of the Bolometer diagnostic for steady-state operation of the W7-X stellarator"; Zhang, D. et al.; Review of Scientific Instruments, Jan 1st, 2010; DOI:10.1063/1.3483194
- "The bolometer diagnostic at stellarator Wendelstein 7-X and its first results in the initial campaign"; D. Zhang, et al. and the W7-X Team; Stellarator-New 2017
- "A low noise highly integrated bolometer array for absolute measurement of VUV and soft x radiation"; K. F. Mast et. al; Review of Scientific Instruments 62, 744 (1991); DOI: 10.1063/1.11.42078
- "Steepest descent moment method for three dimensional magnetohydrodynamic equilibria"; Hirshman, S.P. et al.; Physics of Fluids 26, 3553, (1983); DOI: 10.1063/1.864116
- "Tokamaks"; Wesson, J.; Clarendon Press, Oxford; 1987

Bibliography

- "Numerical investigation of plasma edge transport and limiter heat fluxes in Wendelstein 7-X startup plasmas with EMC3-EIRENE"; Effenberg, F., Feng, Y. et al. Nucl. Fusion 57 (2017) 036021 (15pp); DOI: 10.1088/1741-4326/aa4f83
- "Derivation of bolometer equations relevant to operation in fusion experiments"; Gianone, L. et al.; Review of Scientific Instruments; 20th of November, 2002; DOI: 10.1063/1.1498906
- "Results of the bolometer diagnostic at OP 1.a of W7-X"; internal review of the physics plan during the second operational phase at the stellarator W7-X; 28.02.20i18
- "Characterization of energy confinement in net-current free plasmas using the extended International Stellarator Database"; H. Yamada et al.; INSTITUTE OF PHYSICS PUBLISHING and INTERNATIONAL ATOMIC ENERGY AGENCY; Nucl. Fusion 45 (2005) 1684¿1693

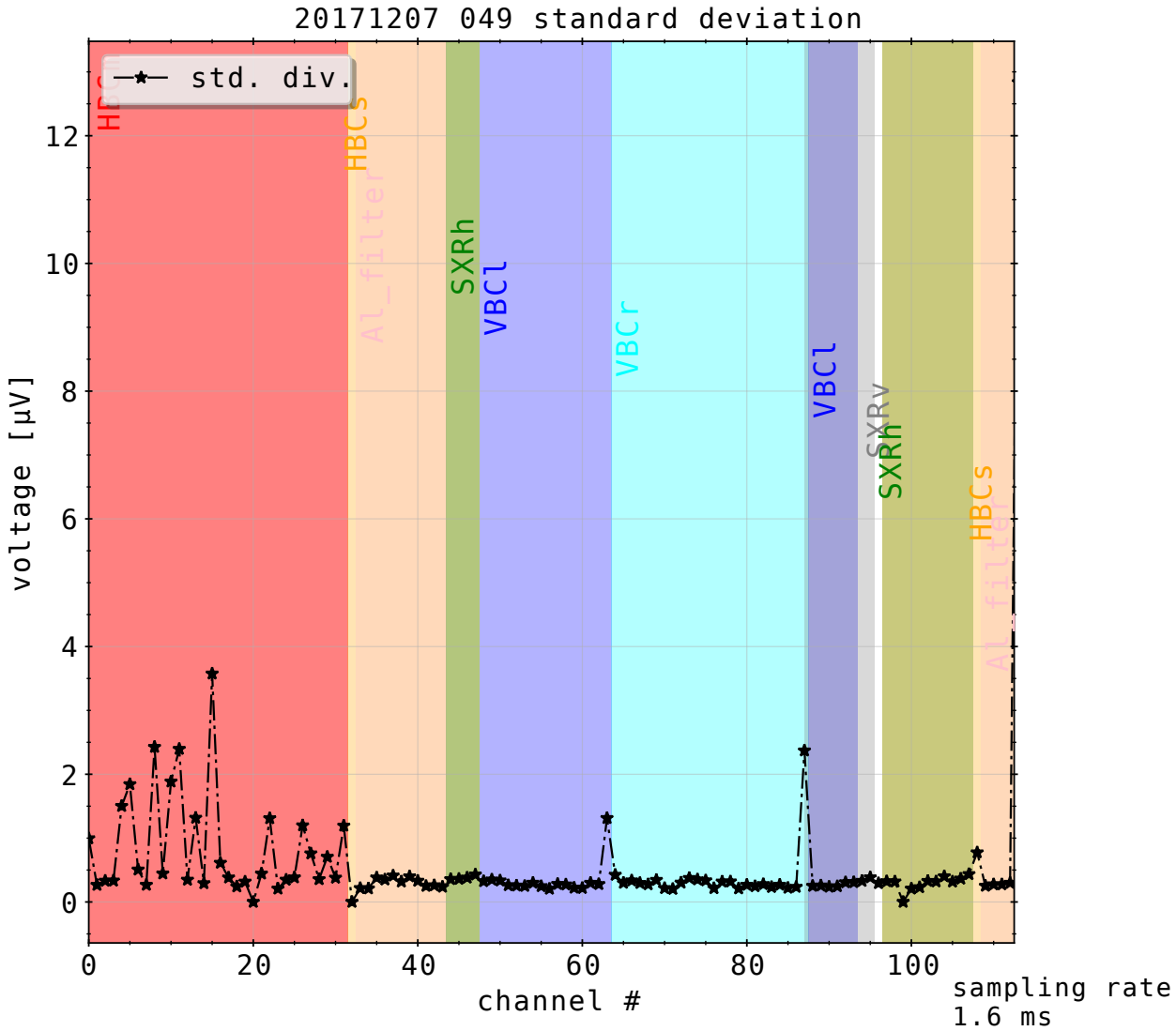
20171207 049 standard deviation
std. div.
HBCs
Al_filter
SXRh
VBCl
VBCr
VBCl
SXRv
SXRh
HBCs
Al_filter
voltage [µV]
channel #
sampling rate
1.6 ms
0
2
4
6
8
10
12
0
20
40
60
80
100

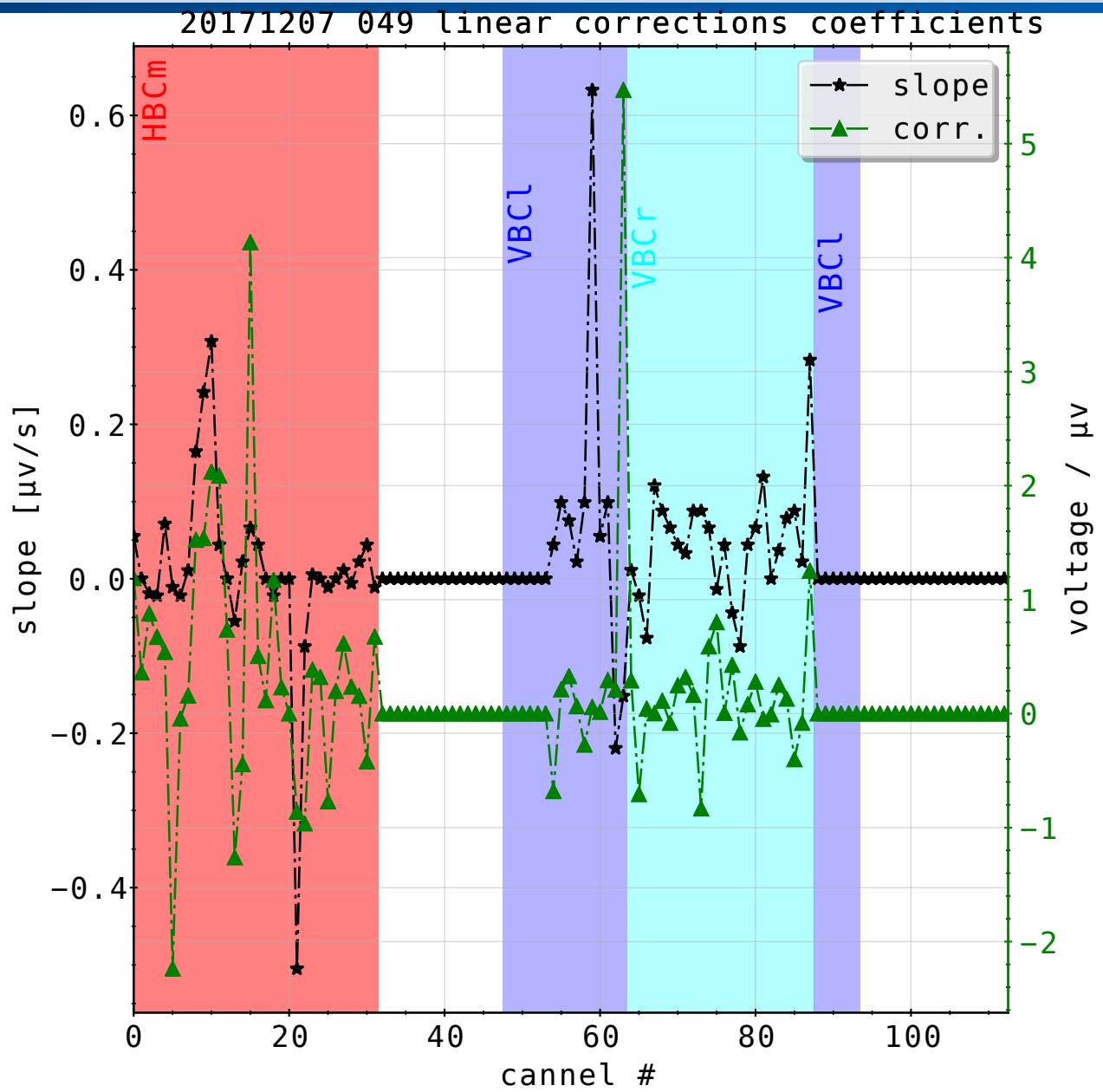
20171207 049 linear corrections coefficients
HBCm
VBCl
VBCr
VBCl
slope
corr.
slope [µv/s]
voltage / µv
cannel #
0.6
0.4
0.2
0.0
−0.2
−0.4
5
4
3
2
1
0
−1
−2
0
20
40
60
80
100

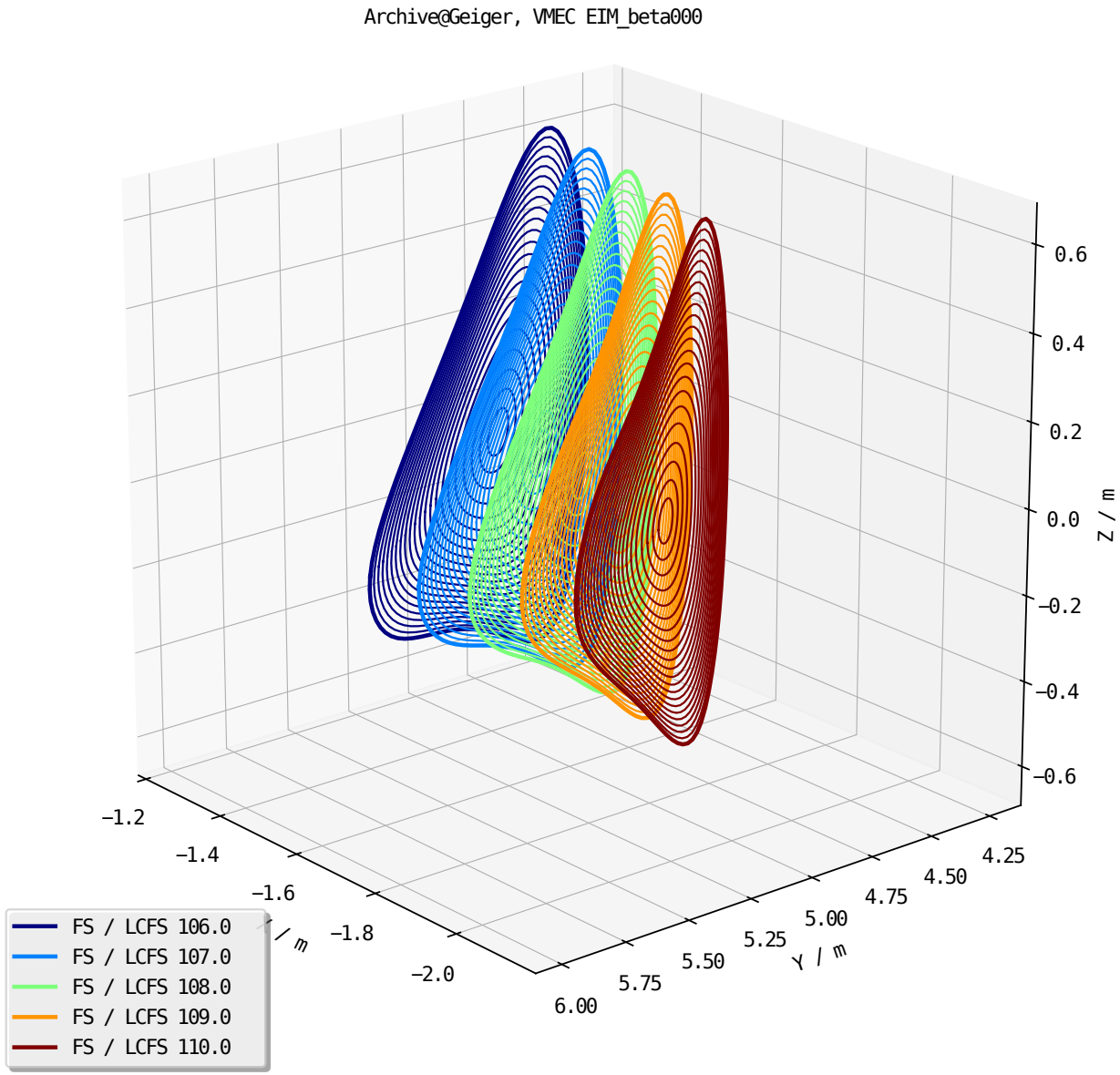
Archive@Geiger, VMEC EIM_beta000
FS / LCFS 106.0
FS / LCFS 107.0
FS / LCFS 108.0
FS / LCFS 109.0
FS / LCFS 110.0
X / m
−1.2
−1.4
−1.6
−1.8
−2.0
Y / m
4.25
4.50
4.75
5.00
5.25
5.50
5.75
6.00
Z / m
0.6
0.4
0.2
0.0
−0.2
−0.4
−0.6

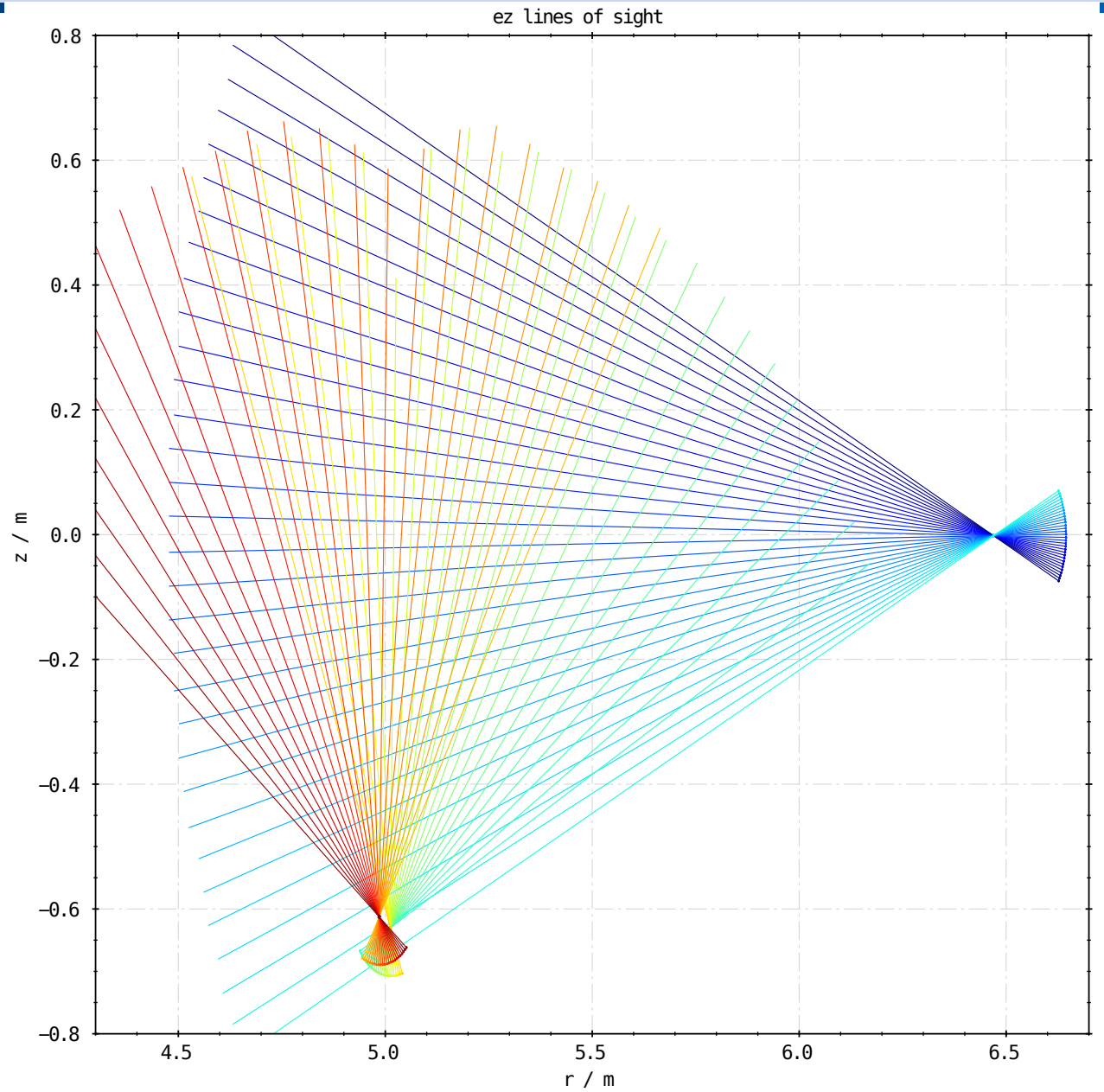
ez lines of sight
0.8
0.6
0.4
0.2
0.0
−0.2
−0.4
−0.6
−0.8
z / m
4.5
5.0
5.5
6.0
6.5
r / m

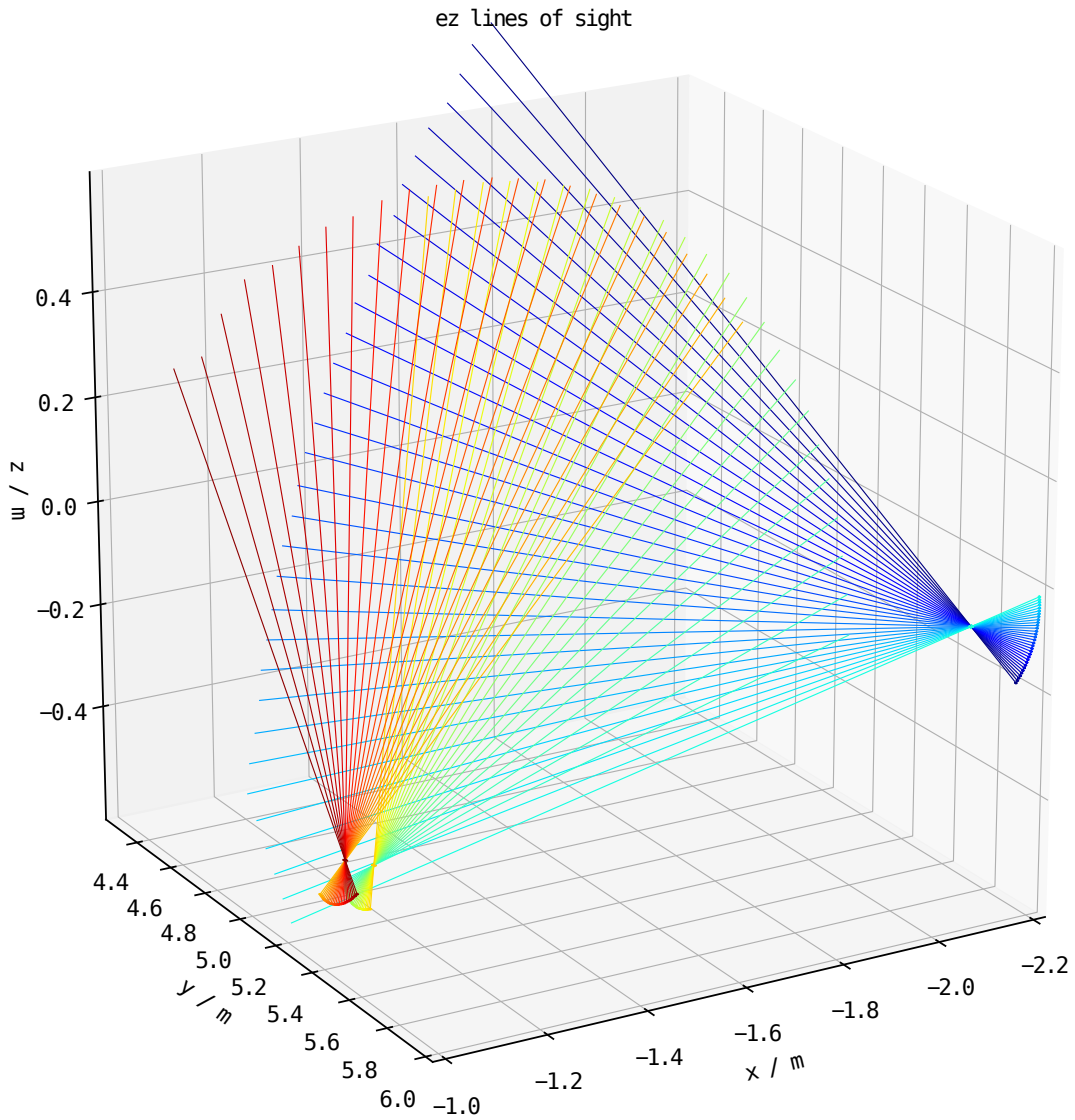
ez lines of sight
0.4
0.2
0.0
−0.2
−0.4
w / z
4.4
4.6
4.8
5.0
5.2
5.4
5.6
5.8
6.0
y / m
−1.0
−1.2
−1.4
−1.6
−1.8
−2.0
−2.2
x / m

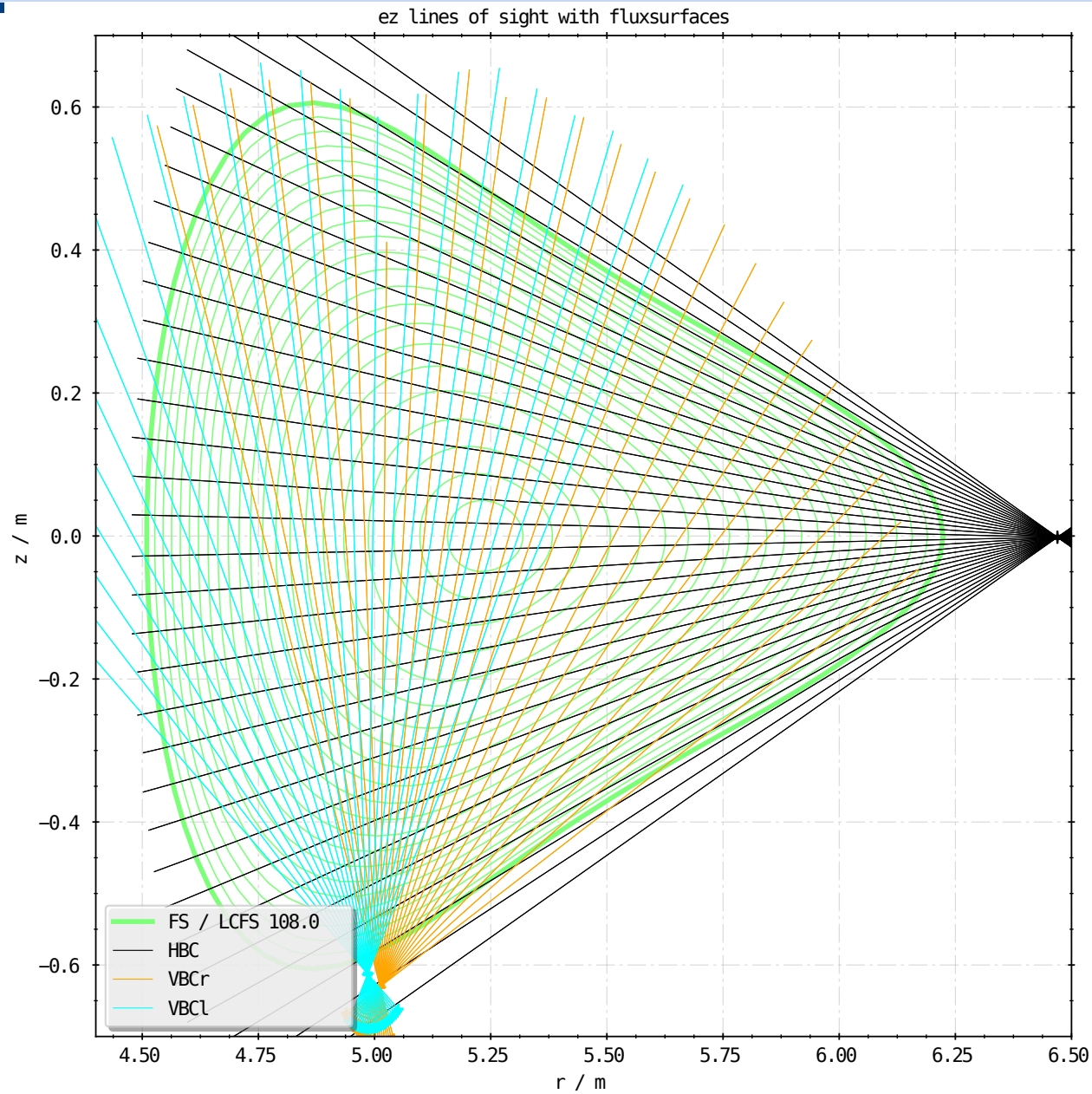
ez lines of sight with fluxsurfaces
0.6
0.4
0.2
0.0
−0.2
−0.4
−0.6
z / m
4.50
4.75
5.00
5.25
5.50
5.75
6.00
6.25
6.50
r / m
FS / LCFS 108.0
HBC
VBCr
VBCl

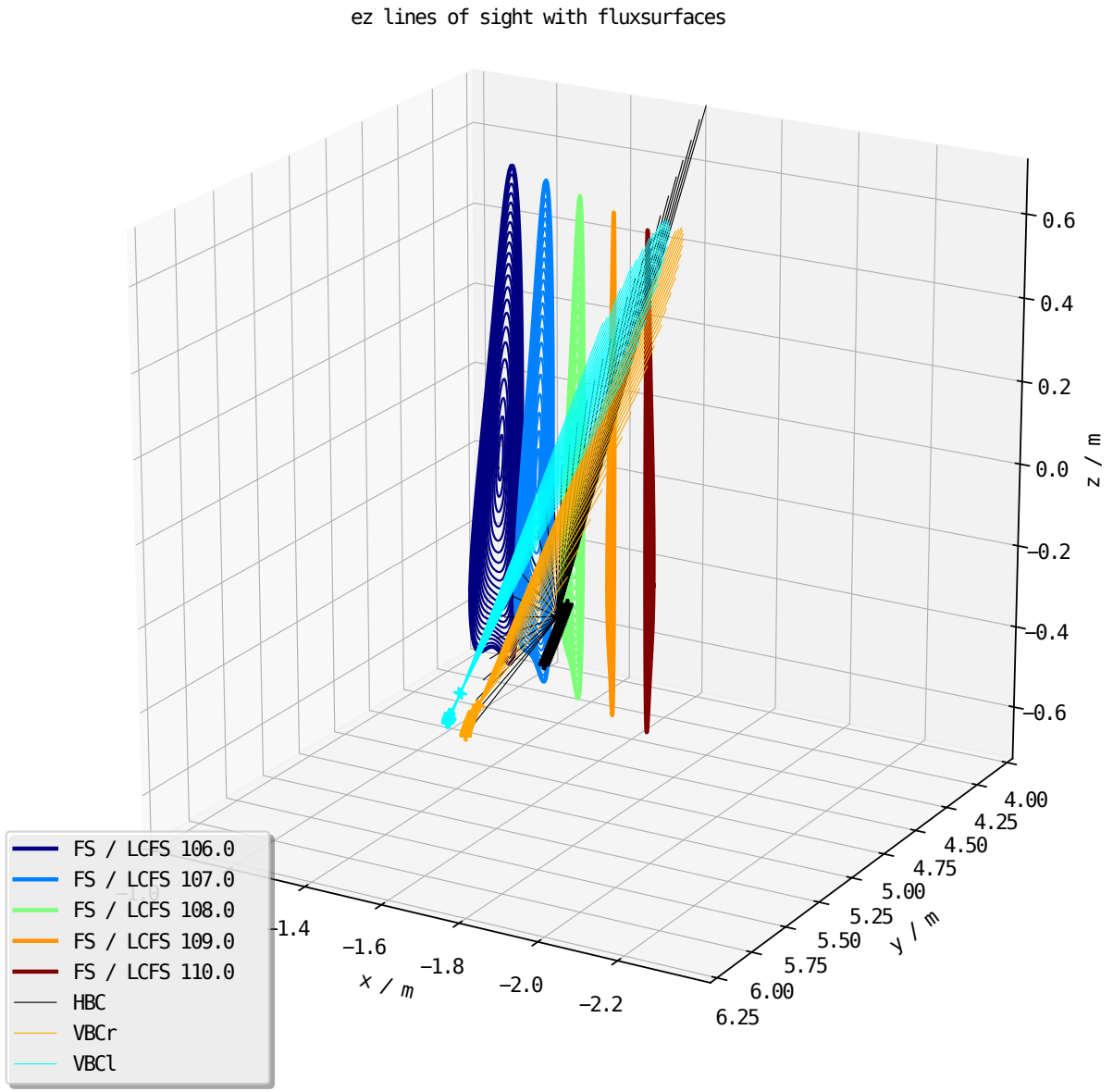
ez lines of sight with fluxsurfaces
FS / LCFS 106.0
FS / LCFS 107.0
FS / LCFS 108.0
FS / LCFS 109.0
FS / LCFS 110.0
HBC
VBCr
VBCl
x / m
y / m
z / m

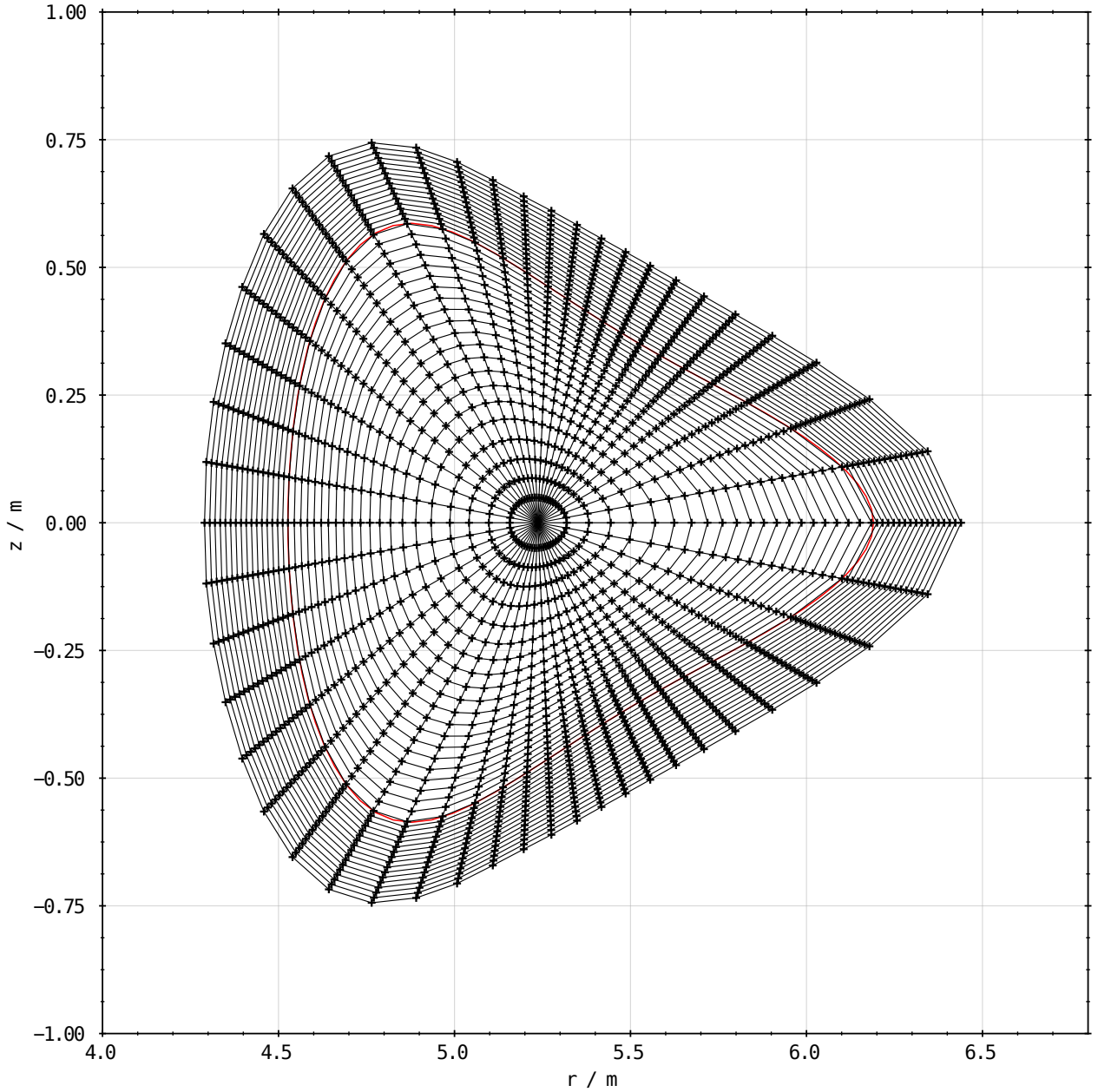
1.00
0.75
0.50
0.25
0.00
−0.25
−0.50
−0.75
−1.00
z / m
4.0
4.5
5.0
5.5
6.0
6.5
r / m

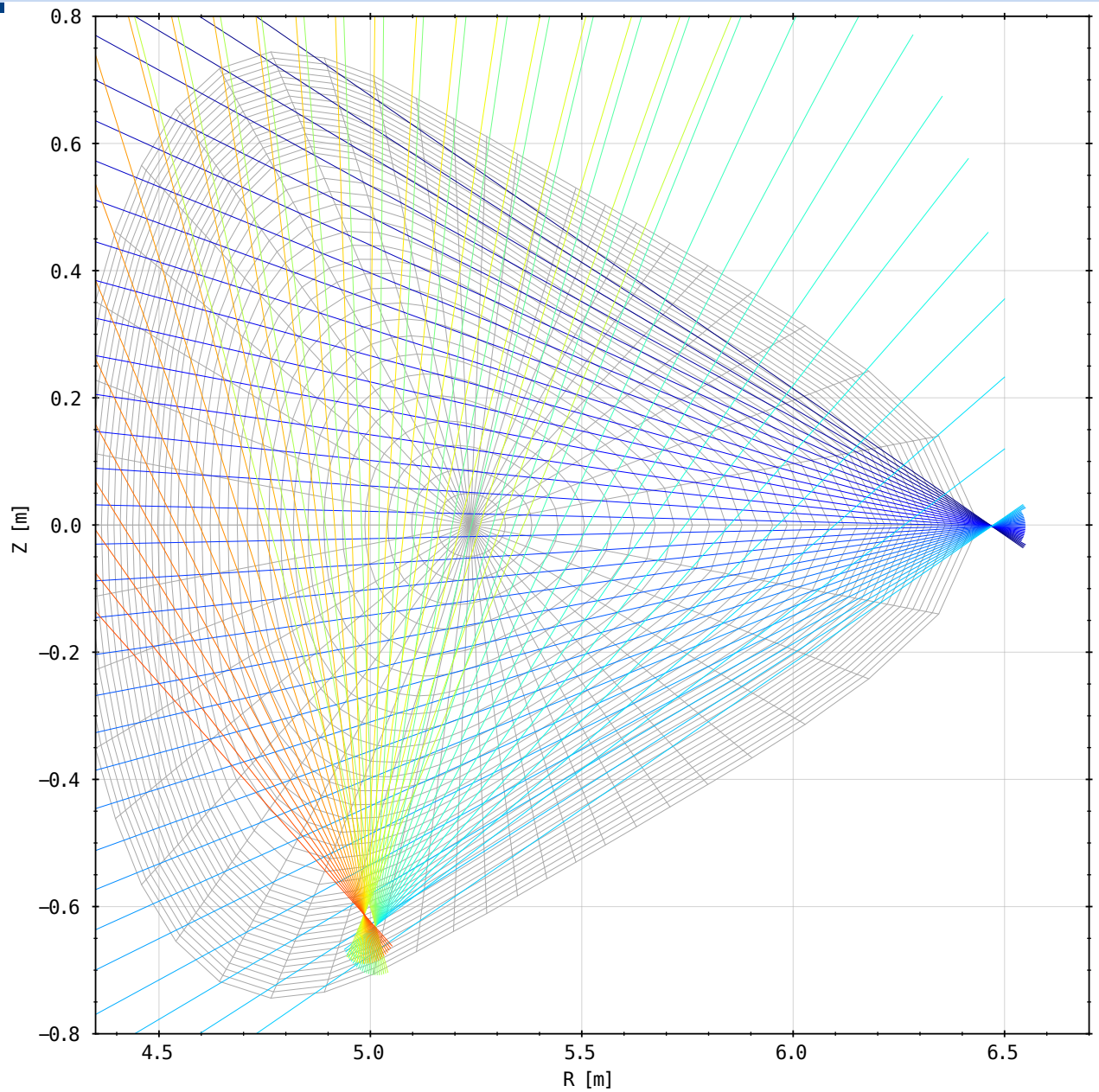
0.8
0.6
0.4
0.2
0.0
−0.2
−0.4
−0.6
−0.8
Z [m]
4.5
5.0
5.5
6.0
6.5
R [m]

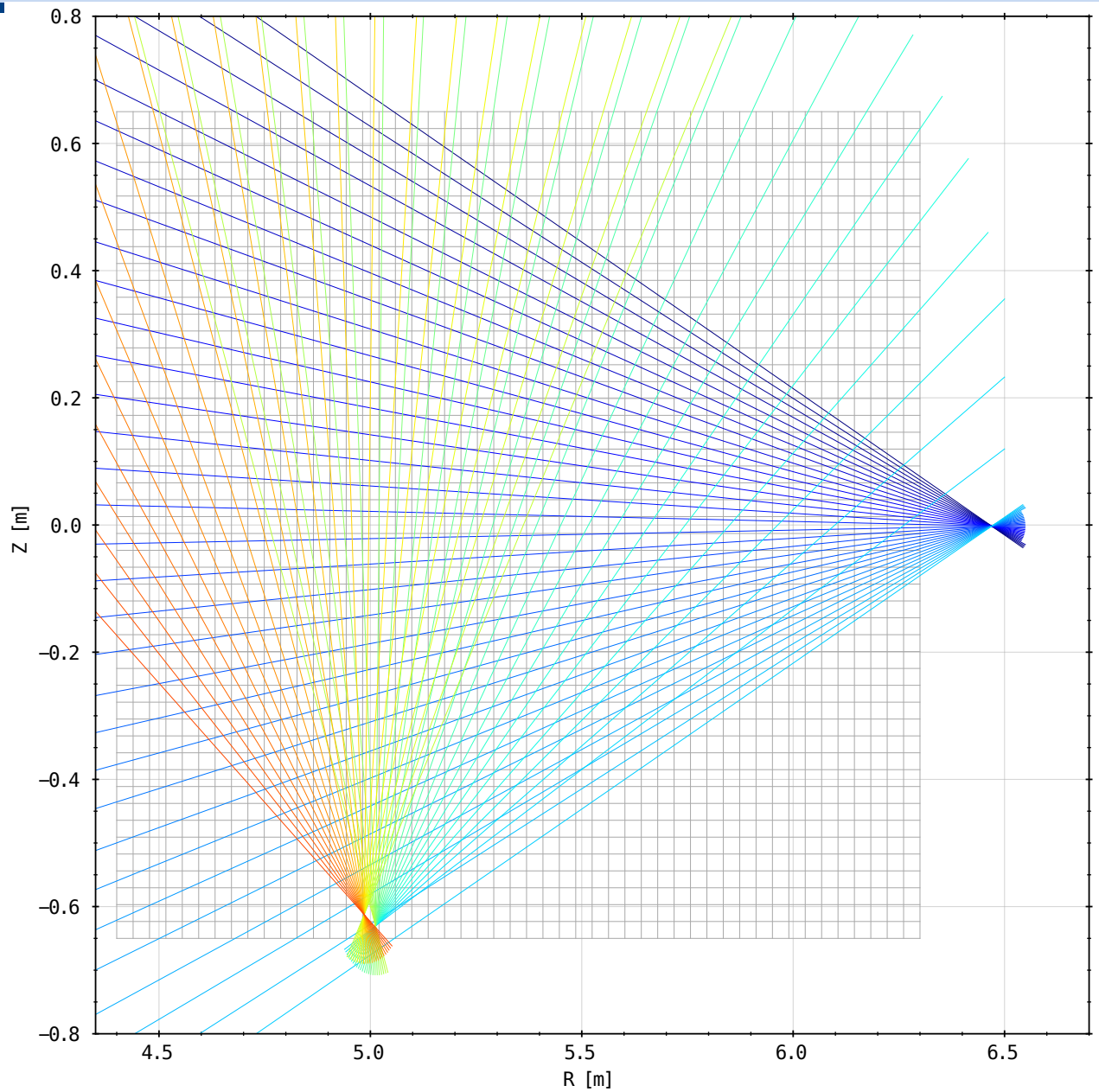
0.8
0.6
0.4
0.2
0.0
−0.2
−0.4
−0.6
−0.8
Z [m]
4.5
5.0
5.5
6.0
6.5
R [m]

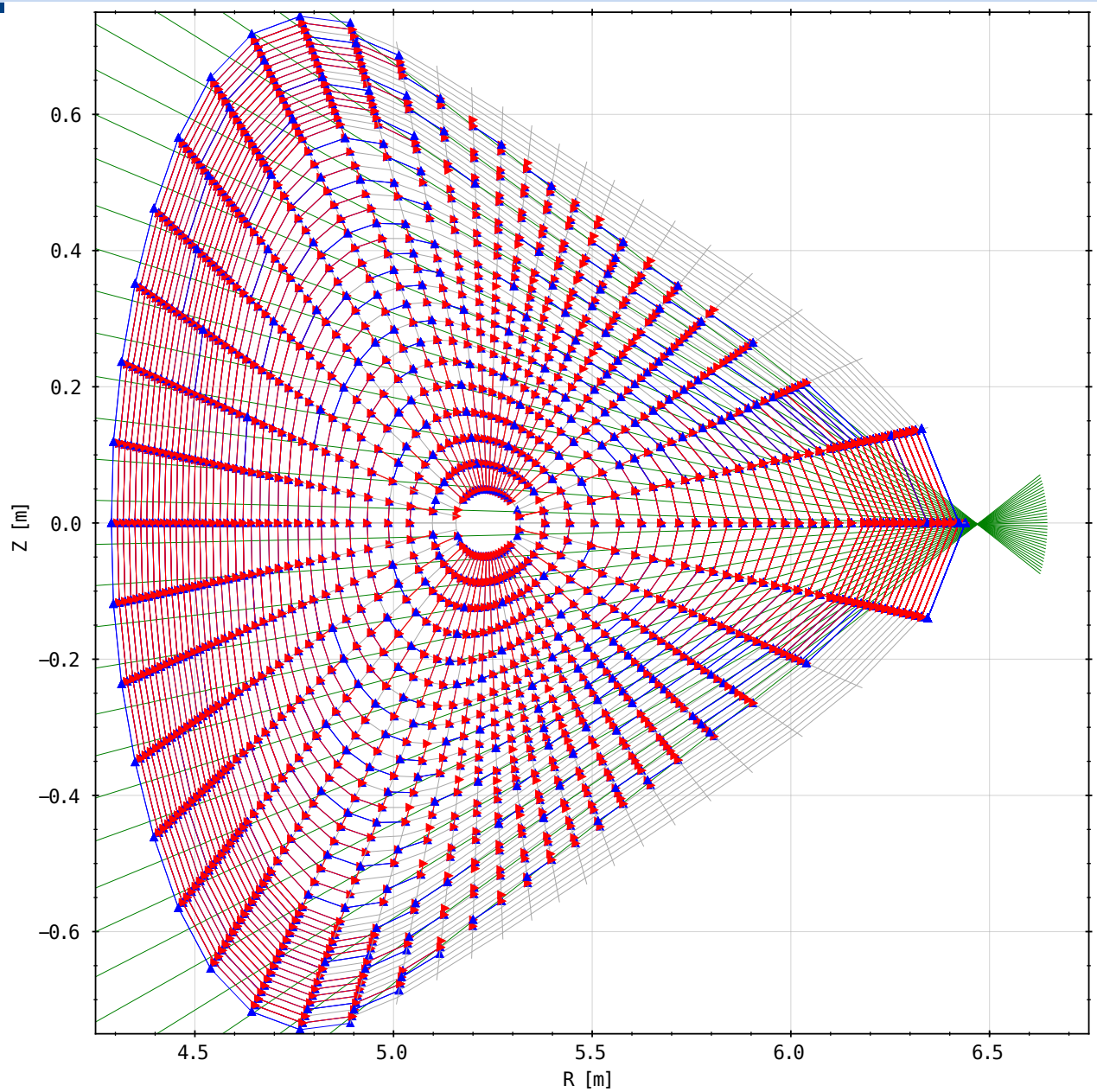
0.6
0.4
0.2
0.0
−0.2
−0.4
−0.6
Z [m]
4.5
5.0
5.5
6.0
6.5
R [m]

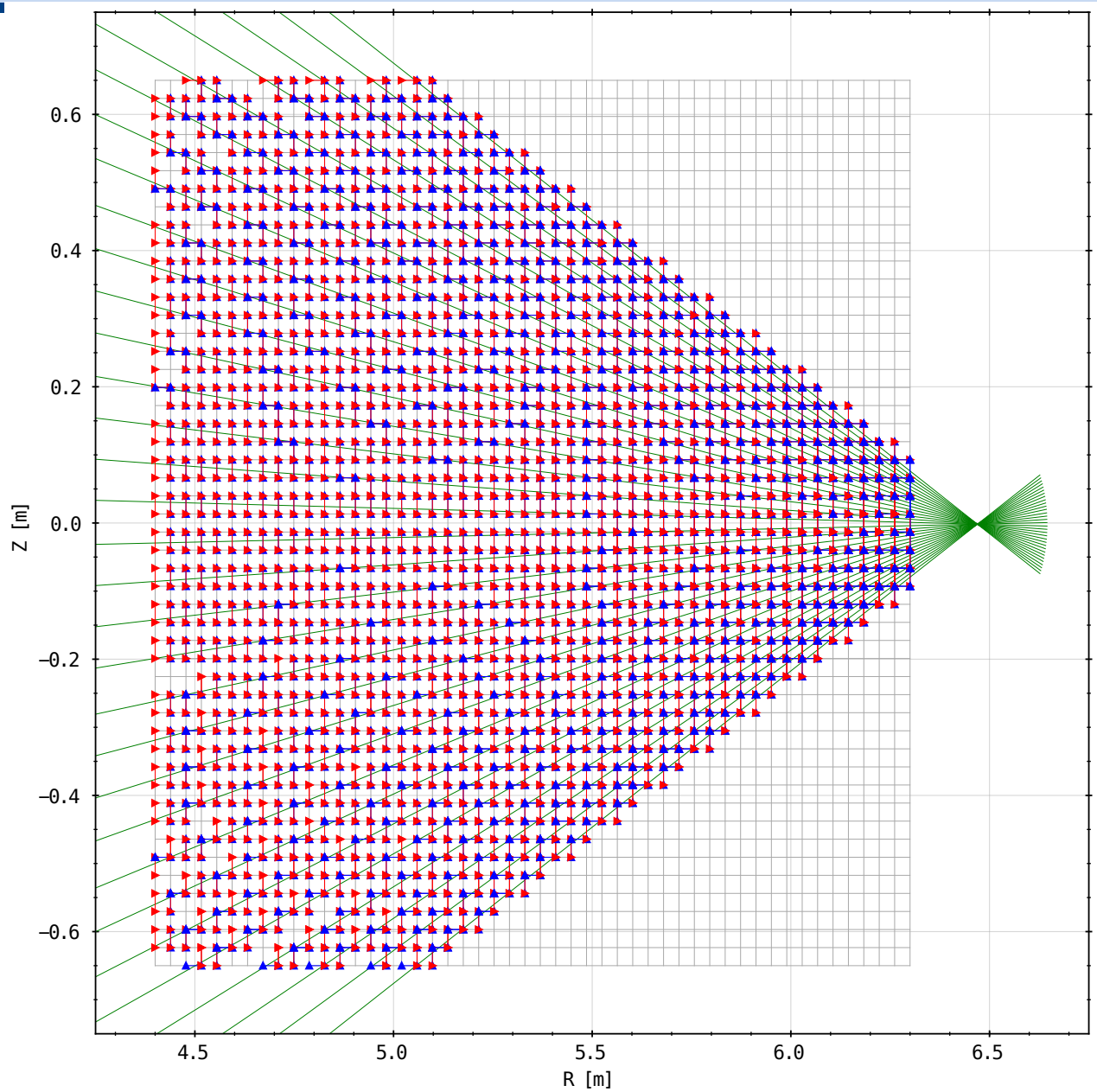
0.6
0.4
0.2
0.0
−0.2
−0.4
−0.6
Z [m]
4.5
5.0
5.5
6.0
6.5
R [m]